Science and Technology Indonesia
e-ISSN:2580-4391 *p*-ISSN:2580-4405
Vol. 10, No. 3, July 2025

Research Paper

Citrus hystrix DC. Peel Essential Oil Protects Mice from UVB-Induced Skin Damage through Antioxidant and Immunomodulatory Properties

Tran Thi Phuong Nhung[1], Le Pham Tan Quoc[1*]

[1]*Institute of Biotechnology and Food Technology, Industrial University of Ho Chi Minh City, Ho Chi Minh City, 700000, Vietnam*
***Corresponding author**: lephamtanquoc@iuh.edu.vn*

Abstract
This study evaluated the protective effects of *Citrus hystrix* peel essential oil (EOCH) against UVB-induced skin damage in mice. The mice were randomly divided into six groups: a normal control, a UVB-exposed group, a UVB+VAP group, and three EOCH-treated groups receiving 1%, 5%, or 10% EOCH. UVB exposure was applied for 4 weeks to induce skin damage. Skin damage was assessed by scoring lesions and measuring moisture levels, while oxidative stress was evaluated by determining malondialdehyde (MDA) and hydrogen peroxide (H_2O_2) levels in the organs. The antioxidant defense was analyzed via the activities of glutathione peroxidase (GPx), glutathione reductase (GR), and thioredoxin reductase (TRx), along with the GSH/GSSG ratio. Immune response was assessed by measuring white blood cell (WBC) counts and evaluating phagocytic activity. UVB exposure increased skin damage scores to 3.6±0.55 and reduced moisture from 34.88±0.83% to 16.61±0.53% ($p < 0.05$). In contrast, the EOCH10 group restored damage scores to 0 and moisture levels to 31.85±0.34% ($p < 0.05$ vs. UVB). EOCH10 also significantly lowered MDA and H_2O_2 levels and enhanced antioxidant enzyme activities. Moreover, immune parameters were improved, with WBC counts, PR, and PI showing significant recovery ($p < 0.05$). Overall, EOCH demonstrated comprehensive protective effects against UVB-induced skin damage, supporting its potential as a natural therapeutic agent.

Keywords
Immunomodulatory Effects, Natural Skincare, Photodamage, Skin Protection

Received: 5 January 2025, Accepted: 14 April 2025
https://doi.org/10.26554/sti.2025.10.3.741-752

1. INTRODUCTION

Sunlight plays a crucial role in various biological processes; however, excessive exposure to ultraviolet B (UVB, 280–320 nm) radiation causes severe skin damage. Due to its high energy, UVB penetrates the epidermis and triggers a cascade of biochemical reactions that compromise the structural and functional integrity of the skin (Al-Sadek and Yusuf, 2024). One of the primary mechanisms of UVB-induced skin damage is the generation of reactive oxygen species (ROS), which leads to oxidative stress and damage to essential cellular components, including cell membranes, proteins, and DNA (Wei et al., 2024). In parallel, UVB exposure stimulates an inflammatory response by upregulating the production of pro-inflammatory cytokines such as IL-1β, IL-6, and TNF-α, disrupting local immune homeostasis and weakening the skin barrier (Mardiyanto et al., 2020). Recent studies have also linked UVB exposure to ferroptosis-mediated cell death and lipid peroxidation, revealing new pathways of photodamage in skin tissue (Zhang et al., 2023). Additionally, UVB-induced immunosuppression at local and systemic levels increases susceptibility to skin infections and other dermatological disorders (Dourmishev and Guleva, 2021). The consequences of UVB-induced skin damage range from premature skin aging, dermatitis, and sunburn to actinic keratosis and skin cancer (Al-Sadek and Yusuf, 2024). Prolonged UVB exposure induces genetic mutations in skin cells, increasing the risk of non-melanoma skin cancers such as basal cell carcinoma (BCC) and squamous cell carcinoma (SCC) (Fan et al., 2023). Emerging evidence also suggests that UVB can disrupt skin microbiota composition, further compromising skin immunity and accelerating inflammation (Xu et al., 2024). Given these detrimental effects, there is an urgent need for effective skin protection strategies, particularly those derived from natural compounds.

In this context, antioxidants and immunomodulatory compounds play a crucial role in mitigating UVB-induced damage. Antioxidants such as polyphenols, flavonoids, and terpenoids scavenge ROS, reducing oxidative stress and protecting skin cells from damage (Chaudhary et al., 2023). Simultaneously, immunomodulatory compounds regulate inflammatory responses, maintain the integrity of the skin barrier, and coun-

teract UVB-induced immunosuppression (He et al., 2024). Novel research has highlighted that plant-derived exosomes and nano-formulated polyphenols exhibit superior bioavailability and efficacy in protecting the skin against UVB (Yang et al., 2023b; Nunes et al., 2025). Consequently, the investigation and development of natural compounds with antioxidant and immunomodulatory properties present a promising approach to safeguarding the skin against UVB-induced damage.

Citrus hystrix DC., a species belonging to the Rutaceae family, is well known for its high essential oil content in the fruit peel and has been widely utilized in traditional medicine and the food industry (Siti et al., 2022). The major constituents of *Citrus hystrix* peel essential oil include limonene, citronellal, flavonoids, polyphenols, and various monoterpenoids (Long et al., 2023). Among these, limonene exhibits intense antioxidant activity, effectively scavenging free radicals and protecting skin cells from oxidative stress. Citronellal possesses anti-inflammatory and antimicrobial properties, contributing to inflammation reduction and protection against skin infections. Additionally, flavonoids and polyphenols serve as key antioxidants that safeguard cellular membranes and DNA from UVB-induced damage. Furthermore, other monoterpenoids present in the essential oil support tissue regeneration, modulate immune responses, and maintain skin barrier integrity (Nuryandani et al., 2024). Previous studies have demonstrated that essential oils from various Citrus species exhibit protective effects against UVB-induced skin damage through antioxidant and anti-inflammatory mechanisms. Li et al. (2024) reported that *Citrus paradisi*, *Fortunella crassifolia*, *Citrus sinensis*, and *Citrus reticulata* peel essential oils mitigate oxidative stress and UVB-induced dermatitis by modulating the activity of antioxidant enzymes such as superoxide dismutase (SOD) and catalase. Similarly, research by Ghani et al. (2021) demonstrated that grapefruit (Citrus × paradisi var. red blush) peel essential oil protects human skin cells from UVB-induced DNA damage by reducing malondialdehyde (MDA) levels and enhancing glutathione (GSH) activity. Moreover, Ayubi et al. (2023) investigated lemon (*Citrus limon*) peel essential oil and found its immunomodulatory and anti-inflammatory effects, which were evidenced by the suppression of pro-inflammatory cytokines, including IL-1β, IL-6, and TNF-α, in a UVB-induced skin damage model in mice. More recently, Fernando et al. (2024) identified that nanoemulsions formulated from Citrus essential oils not only enhance dermal penetration but also significantly reduce UVB-induced erythema and histopathological alterations in mouse skin.

Despite evidence supporting the antioxidant and anti-inflammatory effects of Citrus essential oils against UVB damage, the protective potential of *Citrus hystrix* peel essential oil remains unexplored. No studies have evaluated its effects on UVB-induced skin damage in mice or its mechanisms of action through oxidative stress balance and immune modulation. This study investigates the protective effects of *Citrus hystrix* peel essential oil against UVB-induced skin damage, focusing on antioxidant and immunomodulatory mechanisms. Using a Swiss albino mouse model, it examines skin damage, oxidative stress, inflammation, and cytokine expression. Findings will provide scientific evidence for *Citrus hystrix* as a natural skin protectant, supporting its potential use in plant-based skincare and cosmeceuticals for safe and effective UVB protection.

2. EXPERIMENTAL SECTION

2.1 Chemicals and Reagents

The study used high-quality reagents from reputable manufacturers. *Citrus hystrix* DC. peel essential oil was extracted via steam distillation, while hexane (HPLC-grade, Sigma-Aldrich, USA), ethanol (Merck, Germany), and methanol (Fisher Scientific, USA) were used as solvents. Antioxidant assays employed DPPH and ABTS (Sigma-Aldrich, USA) with Trolox and gallic acid (Sigma-Aldrich, USA) as standards, and sodium carbonate (Merck, Germany) with phosphate-buffered saline (Gibco, USA) as buffers. For in vivo experiments, ketamine (Zoetis, USA) and xylazine (Bayer, Germany) were used for anesthesia, and 10% formalin (Merck, Germany) and H&E staining (Sigma-Aldrich, USA) were used for tissue fixation and analysis. Additional reagents included Triton X-100 and Tween-20 (Sigma-Aldrich, USA), 70% ethanol (Merck, Germany), and ELISA kits for cytokines (R&D Systems, USA). Instrumentation comprised a UVB lamp (UV Products, USA), a UV-Vis spectrophotometer (Shimadzu, Japan), and HPLC/GC-MS systems (Agilent Technologies, USA).

2.2 Collection and Extraction of Essential Oil From Plant Material

Citrus hystrix DC. fruits were harvested from Tinh Bien District, An Giang Province, Vietnam. The fruits, each weighing approximately 50 - 52 grams, were collected at their optimal ripeness, which is typically reached after a 3-month growth period. For the extraction of essential oil, a steam distillation method was employed due to its efficacy in producing pure oil while preserving sensitive compounds that might be degraded by other techniques. Only fruits with intact and undamaged peels, free from insect infestation, were selected for processing. Following a thorough cleaning, the fruits were air-dried at ambient temperature, and the peels were carefully removed and cut into small pieces. From approximately 24 - 25 kg of fresh fruit, about 9 - 10 kg of peel was obtained, resulting in a total batch yield of 58 - 60 kg of peel. The distillation process was conducted at 100°C for 2 - 3 hours, yielding an essential oil extraction efficiency of roughly 3.1%. The final product designated EOCH, is stored in dark glass containers at room temperature to maintain its quality.

2.3 Extraction and Processing of *P*eel Essential Oil

In this study, EOCH was prepared using the method described by Long et al. (2023). Fresh fruit peels were subjected to hydrodistillation following the detailed standard protocols outlined in their publication. The authors conducted a comprehensive analysis of the resulting oil, meticulously characterizing

Table 1. The Draize Scoring System for Evaluating Skin Reactions Involves Separate Assessments for Erythema (Redness) and Edema (Swelling), Each Rated On A Scale From 0 To 4

Score	Erythema (Redness)	Edema (Swelling)
0	No visible redness on the skin	No noticeable swelling
1	Mild erythema (slightly visible, diffuse redness)	Minor edema (barely detectable thickening of the skin)
2	Moderate erythema (distinct and localized redness)	Moderate swelling (clearly evident increase in skin thickness)
3	Severe erythema (marked redness with noticeable swelling)	Pronounced edema (skin visibly raised or swollen)
4	Extremely severe erythema (deep red, possibly with tissue damage)	Intense edema (skin significantly distended and deformed)

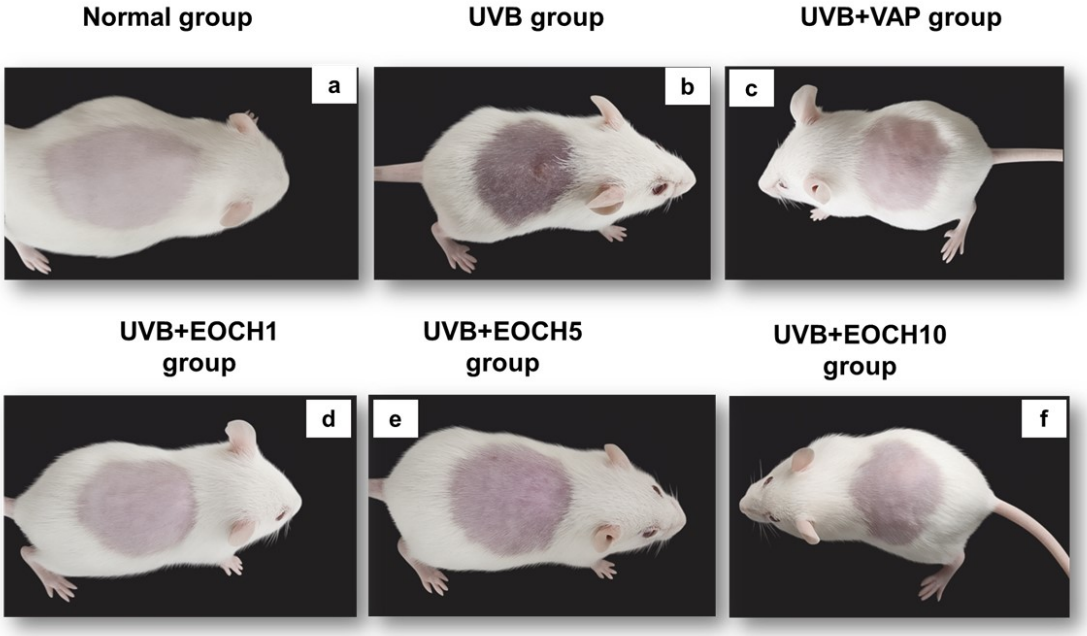

Figure 1. Effects Of C. Hystrix DC. Peel Essential Oil on UVB-induced Skin Damage in Mice. (a) Normal Group with No UVB Exposure. (b) UVB Group Showing Severe Erythema and Skin Damage. (c) UVB+VAP Group Exhibiting Partial Improv-ement. (d-f) Groups Treated With EOCH At Different Concentrations (1%, 5%, and 10%), Showed Varying Degrees of Skin Recovery

its chemical profile - including the identification of volatile constituents and key phytochemical groups. By employing the same extraction procedure, we ensured consistency in the quality of the essential oil, which in turn allows for a direct and meaningful comparison between our current findings and the data reported by Long et al. (2023).

2.4 Experimental Animals

Swiss albino mice with an average body weight of 28-30 g, were obtained from the Pasteur Institute in Ho Chi Minh City, Vietnam. Upon arrival, the animals were housed in glass cages with wood shavings that had been pre-treated with a biological agent to effectively control odors and were allowed to acclimatize for 14 days. During this period, the mice were maintained under strictly controlled environmental conditions, with ambient temperatures kept between 24 and 26°C, relative humidity at 60-62%, and a fixed 12-hour light/dark cycle. They were provided with a specially formulated rodent diet and filtered water available ad libitum. All experimental procedures conformed to the Cioms and Iclas (2012).

2.5 Experimental Design

The mice were randomly divided into six groups, each consisting of five individuals. The Normal group was neither exposed to UVB nor received any treatment, whereas the UVB group was subjected to UVB irradiation without any intervention, serving as the negative control. The UVB+VAP group underwent UVB exposure followed by treatment with 2% vitamin A palmitate, serving as the positive control. Meanwhile, the UVB+EOCH groups were exposed to UVB and treated with

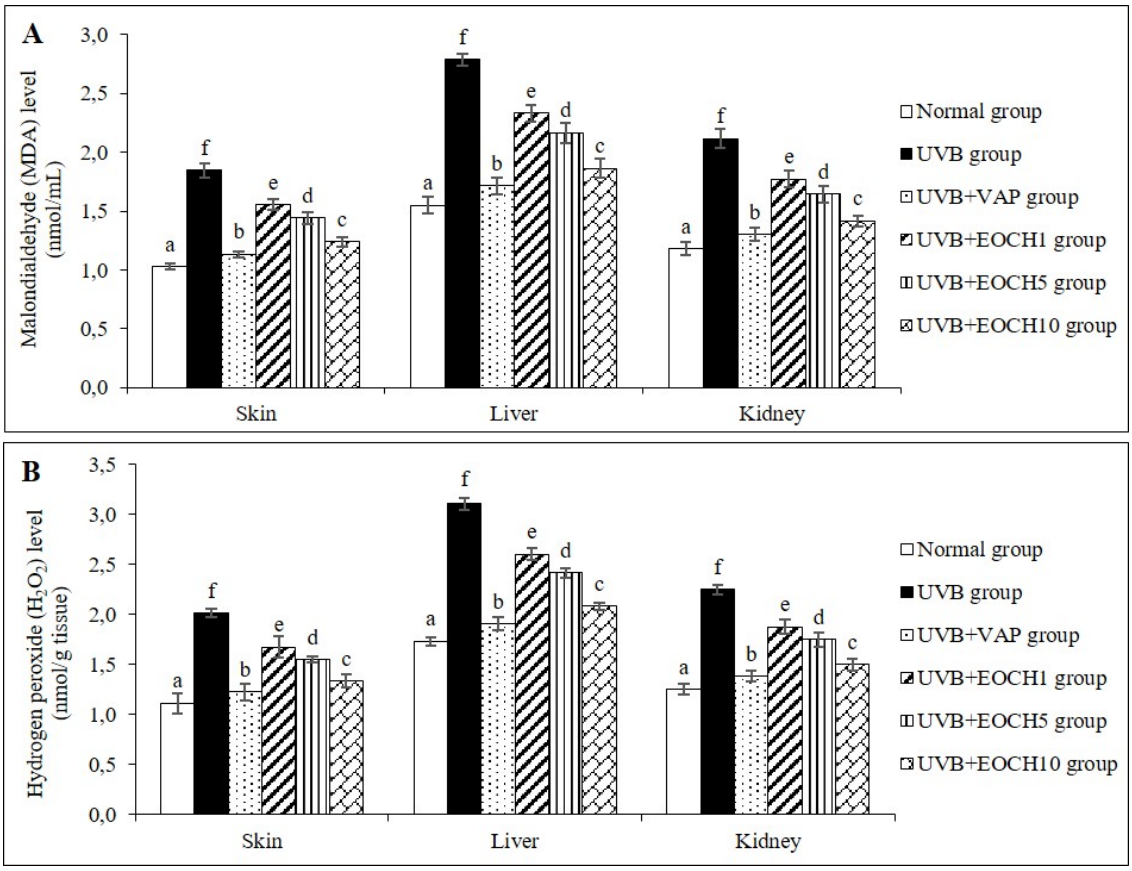

Figure 2. EOCH Treatment Reduced Oxidative Stress in UVB-Induced Skin Damage in Mice. (A) Malondialdehyde (MDA) Levels (Nmol/Ml): This Panel Evaluates Lipid Peroxidation. UVB Exposure Significantly Increased MDA Levels in All Tissues Compared to The Normal Group. Treatment With EOCH (1, 5, and 10 Mg/Kg) or VAP Reduced MDA Levels In A Dose-Dependent Manner, with EOCH10 Showing The Greatest Effect. All Treatment Groups Remained Significantly Different From Both The UVB and Normal Groups ($p < 0.05$). (B) Hydrogen Peroxide (H_2O_2) Levels (Nmol/G Tissue): This Panel Assesses Reactive Oxygen Species Accumulation. UVB Irradiation Elevated H_2O_2 Levels Across All Tissues. Treatment Groups Significantly Decreased H_2O_2 Levels Compared To The UVB Group, Particularly EOCH10. A Dose-Dependent Trend Was Observed, And Statistical Significance Is Indicated By Different Letters (a–f, $p < 0.05$).

Citrus hystrix peel essential oil (EOCH) at concentrations of 1%, 5%, and 10%, designated as UVB+EOCH1, UVB+EOCH5, and UVB+EOCH10, respectively. UVB irradiation was carried out using a CL-1000 M UV lamp (UVP, Upland, CA, USA) with a peak emission at 302 nm. The administered UVB dose ranged from 80 mJ/cm^2, corresponding to an exposure duration of 30 seconds. The lamp was positioned 5 cm above the platform to ensure uniform irradiation. Following UVB exposure, 100 μL of the respective formulation was applied topically once daily for 21 consecutive days.

Throughout the experimental period, weekly assessments were performed that included Draize scoring, visual inspections, and measurements of skin moisture levels. After the study, the mice were first anesthetized by administering an intraperitoneal injection of sodium pentobarbital at a dose of 60 mg/kg, followed by euthanasia via CO_2 inhalation. Subsequently, skin, liver, and kidney tissues were carefully excised, processed, and homogenized. These tissue homogenates were then subjected to biochemical analyses designed to evaluate the antioxidant and immunomodulatory properties of EOCH.

2.6 Procedure for Assessing Skin Irritation (Draize Test)

The evaluation procedure was conducted as described by Lin et al. (2014), with minor modifications to suit the scope of this study. The assessment criteria were based on the Draize scoring system, a standardized method for measuring and evaluating skin irritation, including erythema (redness) and edema (swelling) (Table 1).

2.7 Skin Moisture Measurement Method

Skin hydration was measured using a corneometer CM 825 (Courage + Khazaka, Germany) at predefined sites on the dorsal skin of the mice to ensure consistency. Before measurement, the skin was gently cleansed and allowed to equilibrate at room temperature for at least 10 minutes, minimizing external in-

Table 2. Draize Score Assessment in The Study on The Effectiveness of *Citrus hystrix* Peel Essential Oil in Reducing UVB-induced Skin Damage in Mice

Time	Normal group	UVB group	UVB+VAP group	UVB+EOCH1 group	UVB+EOCH5 group	UVB+EOCH10 group
“"0"“	0.00±0.00^{a}	3.00±0.71^{b}	3.00±0.71^{b}	3.00±0.71^{b}	3.00±0.71^{b}	3.00±0.71^{b}
1 h	0.00±0.00^{a}	3.00±0.00^{c}	2.40±0.55^{b}	2.60±0.55^{bc}	2.60±0.55^{bc}	2.40±0.55^{b}
2 h	0.00±0.00^{a}	3.00±0.00^{c}	2.40±0.55^{b}	2.60±0.55^{bc}	2.40±0.55^{b}	2.40±0.55^{b}
24 h	0.00±0.00^{a}	3.00±0.00^{c}	2.00±0.00^{b}	2.40±0.55^{b}	2.40±0.55^{bc}	2.20±0.45^{b}
48 h	0.00±0.00^{a}	3.00±0.00^{d}	2.00±0.00^{b}	2.40±0.55^{c}	2.20±0.45^{bc}	2.00±0.00^{b}
72 h	0.00±0.00^{a}	3.00±0.00^{c}	1.60±0.55^{b}	2.20±0.84^{b}	1.80±0.45^{b}	1.60±0.55^{b}
5 days	0.00±0.00^{a}	3.20±0.45^{b}	1.40±0.55^{b}	1.80±0.45^{b}	1.60±0.55^{b}	1.40±0.55^{b}
7 days	0.00±0.00^{a}	3.40±0.55^{d}	0.80±0.45^{b}	1.40±0.55^{c}	1.20±0.45^{bc}	0.80±0.45^{b}
2 weeks	0.00±0.00^{a}	3.40±0.55^{c}	0.40±0.55^{a}	1.20±0.45^{c}	1.00±0.00^{b}	0.40±0.55^{a}
4 weeks	0.00±0.00^{a}	3.60±0.55^{c}	0.00±0.00^{a}	1.00±0.00^{c}	0.60±0.55^{b}	0.00±0.00^{a}

Values are expressed as Mean±SD, and letters (a, b, c, and d) represent the difference between groups ($p < 0.05$).

Table 3. Skin Moisture Evaluation in *Citrus hystrix* Peel Essential Oil Treatment for UVB-Induced Skin Damage in Mice

Experimental group	“0”	1 day	3 days	5 days	7 days	2 weeks	4 weeks
Normal group	35.09±0.30^{a}	34.97±0.29^{f}	34.88±0.80^{f}	35.04±0.60^{f}	34.92±0.59^{f}	35.06±0.45^{f}	35.02±0.61^{f}
UVB group	34.88±0.83^{a}	21.80±0.56^{a}	20.52±0.64^{a}	19.38±0.42^{a}	18.36±0.26^{a}	17.44±0.45^{a}	16.61±0.53^{a}
UVB+VAP group	35.07±0.30^{a}	26.98±0.48^{e}	28.06±0.28^{e}	29.23±0.27^{e}	30.50±0.29^{e}	31.88±0.86^{e}	33.40±0.61^{e}
UVB+EOCH1 group	34.92±0.61^{a}	22.53±0.32^{b}	23.28±0.27^{b}	24.08±0.34^{b}	24.94±0.47^{b}	25.87±0.86^{b}	26.86±0.43^{b}
UVB+EOCH5 group	34.98±0.71^{a}	24.12±0.70^{c}	24.99±0.45^{c}	25.91±0.38^{c}	26.91±0.44^{c}	27.98±0.29^{c}	29.15±0.31^{c}
UVB+EOCH10 group	35.04±0.32^{a}	25.96±0.29^{d}	26.95±0.47^{d}	28.03±0.87^{d}	29.20±0.27^{d}	30.47±0.22^{d}	31.85±0.34^{d}

Values are expressed as Mean±SD, and letters (a, b, c, d, e, and f) represent the difference between groups ($p < 0.05$).

fluences. The probe was then applied perpendicularly with light pressure, and three consecutive readings were taken for each mouse. The final hydration value was calculated as the average of these readings to enhance measurement reliability. These measurements were performed weekly throughout the experiment to track changes resulting from UVB exposure and treatment interventions (Fauzi et al., 2022).

2.8 Oxidative Stress and Antioxidant Parameter Analysis

At the end of the experiment, skin, liver, and kidney tissues were collected and immediately stored at –80°C until analysis. The tissues were homogenized in an appropriate buffer using a tissue homogenizer, then centrifuged at 10 000 rpm for 15 minutes at 4°C in a Beckman Coulter Allegra X-12R centrifuge (Beckman Coulter, USA) to obtain the supernatant for biochemical assays. Oxidative stress markers and antioxidant parameters were quantified using standard calibration curves. Lipid peroxidation was measured by assessing malondialdehyde (MDA, nmol/mL) via the TBARS assay, with absorbance recorded at 532 nm using a Shimadzu UV-1800 spectrophotometer (Shimadzu, Japan). Hydrogen peroxide (H_2O_2, nmol/g tissue) levels were determined using a colorimetric reaction with xylenol orange under acidic conditions. The glutathione system was evaluated by measuring reduced glutathione (GSH, µmol/mL) through its reaction with DTNB, producing a yellow chromophore detected at 412 nm. Oxidized glutathione (GSSG, nmol/mg protein) was quantified via enzymatic reduction using NADPH and glutathione reductase, and the GSH/GSSG ratio was calculated to assess redox balance. Enzymatic antioxidant activities were determined by measuring glutathione peroxidase (GPx, U/mg protein) based on NADPH oxidation in a GSH-dependent reaction with H_2O_2, and glutathione reductase (GR, U/mg protein)

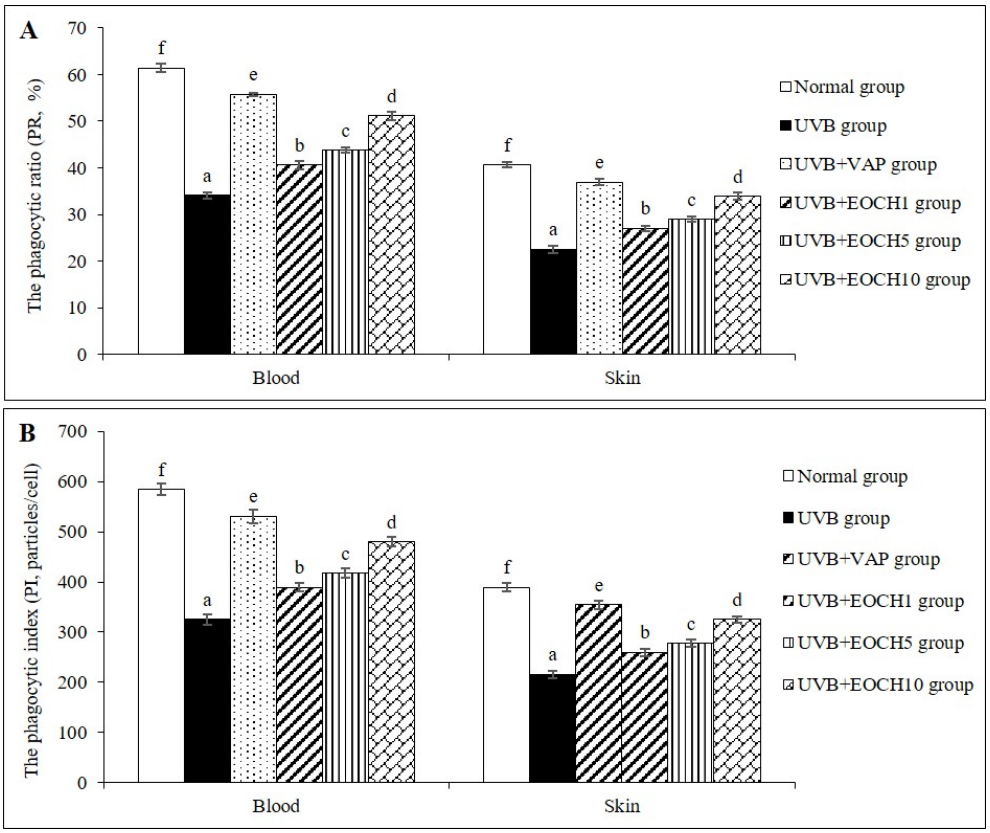

Figure 3. The Effects Of EOCH on Phagocytic Ratio (PR) and Phagocytic Index (PI) in The Blood and Skin Of UVB-Damaged Mice are Shown Below. (A) Phagocytic Ratio (PR, %): UVB Exposure Significantly Reduced The Phagocytic Ratio In Both Blood And Skin, Indicating A Suppressed Immune Response. Treatment with VAP And EOCH At All Tested Doses (1, 5, And 10 Mg/Kg) Improved PR Compared To The UVB Group. The EOCH10 Group Showed The Most Notable Effect, Nearly Restoring PR to Normal Levels. Statistical Significance is Indicated by Different Letters (a–f, $p < 0.05$). (B) Phagocytic Index (PI, Particles/Cell): UVB Irradiation Markedly Decreased The Phagocytic Index In Both Tissues. All Treatment Groups Showed Significant Increases in PI, With EOCH10 Again Demonstrating The Strongest Effect. A Clear Dose-Dependent Improvement Was Observed Across EOCH-Treated Groups. Statistical Differences are Represented by Different Letters (a–f, $p < 0.05$).

by monitoring NADPH consumption during the reduction of GSSG to GSH. Thioredoxin (TRx, µg/mg protein) levels were quantified using an ELISA assay with specific antibodies (Nhung and Quoc, 2024a).

2.9 Immunomodulatory Assessment

At the end of the experiment, blood and skin samples were collected to evaluate immune responses. Blood was drawn from the tail vein and anticoagulated with heparin. Skin samples were excised from UVB-exposed areas, minced, and digested with collagenase or trypsin to isolate infiltrating immune cells for further analysis. Systemic immune responses were assessed by measuring the white blood cell (WBC) count ($\times 10^3$ cells/mm^3) using either a Neubauer hemocytometer or an automated hematology analyzer. Phagocytic activity was determined by incubating immune cells with fluorescent-labeled latex beads or fluorophore-stained dead bacteria, followed by flow cytometry or fluorescence microscopy to calculate the phagocytic ratio (PR, %) and phagocytic index (PI, particles/cell). Neutrophil oxidative burst was evaluated using the nitroblue tetrazolium (NBT) reduction test. Leukocytes were incubated with NBT and phorbol myristate acetate (PMA), and the percentage of cells reducing NBT to formazan was measured via microscopy or spectrophotometry at 620 nm. Total immunoglobulin (TI, mg/mL) levels in plasma were determined using polyethylene glycol precipitation or ELISA. For skin-infiltrating immune cell analysis, isolated cells were stained with antibodies against markers such as CD45 (leukocytes), CD4 and CD8 (*T lymphocytes*), and F4/80 (macrophages), and then quantified by flow cytometry. *T lymphocytes* were further purified using density gradient separation, stimulated with mitogens (ConA or PHA), and their proliferation was assessed using MTT or BrdU incorporation assays (Nhung and Quoc, 2024b).

2.10 Statistical Analysis

Results are presented as the mean ± standard deviation (SD). Statistical evaluations were carried out using Statgraphics Cen-

Table 4. Effects of *C. hystrix* Peel Essential Oil on Glutathione (GSH), Glutathione Disulfide (GSSG), and GSH/GSSG Ratio in UVB-Induced Skin Damage in Mice

Experimental group	GSH level (μmol/mL)			GSSG level (nmol/mg protein)			GSH/GSSG ratio		
	Skin	Liver	Kidney	Skin	Liver	Kidney	Skin	Liver	Kidney
Normal group	4.34± 0.12^{f}	8.61± 0.13^{f}	6.97± 0.30^{f}	0.39± 0.05^{d}	0.74± 0.11^{e}	0.57± 0.07^{c}	11.16± 1.12^{a}	11.85± 2.10^{a}	12.31± 1.95^{a}
UVB group	2.41± 0.04^{a}	4.78± 0.14^{a}	3.87± 0.17^{a}	0.22± 0.07^{a}	0.41± 0.07^{a}	0.32± 0.07^{a}	11.87± 4.22^{a}	12.12± 2.23^{a}	12.44± 2.26^{a}
UVB+VAP group	3.95± 0.14^{e}	7.83± 0.10^{e}	6.34± 0.11^{e}	0.35± 0.11^{c}	0.67± 0.06^{e}	0.52± 0.11^{c}	12.13± 4.06^{a}	11.82± 1.05^{a}	12.72± 2.91^{a}
UVB+EOCH1 group	2.89± 0.13^{b}	5.74± 0.24^{b}	4.65± 0.18^{c}	0.26± 0.07^{ab}	0.49± 0.08^{ab}	0.38± 0.11^{ab}	12.02± 3.55^{a}	12.04± 2.04^{a}	12.97± 4.01^{a}
UVB+EOCH5 group	3.10± 0.09^{c}	6.15± 0.13^{e}	4.98± 0.12^{b}	0.28± 0.05^{abc}	0.53± 0.04^{b}	0.41± 0.04^{b}	11.40± 2.62^{a}	11.70± 0.80^{a}	12.33± 1.22^{a}
UVB+EOCH10 group	3.62± 0.11^{d}	7.18± 0.08^{a}	5.81± 0.13^{d}	0.33± 0.06^{bcd}	0.62± 0.06^{d}	0.48± 0.06^{b}	11.23± 2.55^{a}	11.62± 1.27^{a}	12.34± 1.60^{a}

Values are expressed as Mean±SD; and letters (a, b, c, d, e, and f) represent the difference between groups ($p < 0.05$).

turion XX software. Group comparisons were performed by one-way analysis of variance (ANOVA), with p-values less than 0.05 considered statistically significant.

3. RESULTS AND DISCUSSION

3.1 Phytochemical Composition of Citrus hystrix Peel Essential Oil

Based on the findings of Long et al. (2023), the phytochemical profile of Citrus hystrix peel essential oil (EOCH) comprises 22 volatile compounds, accounting for 99.98% of the total oil content. EOCH is predominantly composed of monoterpenes (both hydrocarbons and monoterpenoids), with a smaller fraction of sesquiterpenes. Notable bioactive constituents identified include germacrene D, camphene, and caryophyllene, which underscore EOCH's potential for applications in food, healthcare, and dermatological products. These compounds play key roles in protecting the skin against UVB-induced damage. Specifically, they can neutralize free radicals generated during UVB exposure, reduce oxidative stress by lowering levels of malondialdehyde (MDA) and hydrogen peroxide (H_2O_2), and support skin integrity by restoring the activities of endogenous antioxidant enzymes such as glutathione peroxidase (GPx), glutathione reductase (GR), and thioredoxin reductase (TRx) (Basholli-Salihu et al., 2017). Moreover, certain terpenes in EOCH have demonstrated immunomodulatory effects (Stasiłowicz-Krzemień et al., 2024). Caryophyllene, a sesquiterpene known for its anti-inflammatory activity, reduces excessive leukocyte infiltration and improves immune parameters such as the phagocytic ratio (PR) and phagocytic index (PI) (Gushiken et al., 2022). Additionally, camphene and germacrene D exhibit antimicrobial and skin-conditioning properties, which help preserve skin hydration and barrier function, mitigating the dehydrating effects of UVB exposure (Kim and Hong, 2024).

Several international studies have also demonstrated the skin-protective properties of herbal essential oils against UVB-induced damage, consistent with the findings observed for EOCH. For instance, a study by Kaur and Saraf (2010) evaluated the UV absorption abilities of various volatile and non-volatile oils, revealing that olive oil had the highest SPF among fixed oils, while peppermint oil ranked highest among essential oils. A review by Li et al. (2023) emphasized that aromatic-ring-containing compounds, such as flavonoids and polyphenols, not only act as natural UV filters but also exert antioxidant and anti-inflammatory activities that reduce the risk of sunburn. Furthermore, Lohani and Morganti (2022) demonstrated that formulations containing geranium and calendula essential oils preserved the skin's antioxidant system by maintaining superoxide dismutase, catalase, total protein, ascorbic acid, and hydroxyproline levels while decreasing MDA levels after UVB exposure. Collectively, these studies confirm the therapeutic potential of EOCH and other botanical essential oils in preventing UVB-induced skin damage.

3.2 Assessment of the Protective Effects of EOCH on UVB-induced Skin Damage in Mice Using Draize Scoring and Visual Evaluation

Table 2 summarizes the draize scores for UVB-induced skin damage in mice and the protective effects of EOCH over time. The normal group maintained a constant score of 0, indicating no irritation. In contrast, the UVB group experienced progressive skin damage, with scores rising to 3.60±0.55 at 4 weeks ($p < 0.05$ vs. normal). The UVB + VAP group showed improvement, with scores declining from 3.00±0.71 initially to 0.00±0.00 at 4 weeks ($p < 0.05$ vs. UVB). Similarly, EOCH

treatment led to dose-dependent recovery: EOCH1 (1%) reduced scores to 1.00±0.00, EOCH5 (5%) to 0.60±0.55, and EOCH10 (10%) achieved near-complete recovery with scores of 0.00±0.00 at 4 weeks (all $p < 0.05$ vs. UVB).

Figure 1 visually confirms these findings. The normal group (Figure 1a) displays smooth, intact skin, while the UVB group (Figure 1b) shows severe erythema, inflammation, and lesions. The UVB + VAP group (Figure 1c) exhibits moderate improvement with reduced redness. Among the EOCH-treated groups, EOCH1 (Figure 1d) shows mild improvement, EOCH5 (Figure 1e) demonstrates a more pronounced reduction in inflammation and lesions, and EOCH10 (Figure 1f) reveals near-complete skin recovery, closely resembling the normal group.

The evaluation of EOCH against UVB-induced skin damage in mice, using Draize scoring and visual assessment, reveals its strong, dose-dependent protective effects. UVB exposure caused severe erythema, inflammation, and lesions (Yang et al., 2023a), while EOCH treatment gradually reduced these symptoms; the highest concentration nearly restored the skin to its normal appearance. This protective effect is largely attributed to EOCH's rich phytochemical profile - particularly monoterpenes and sesquiterpenes such as germacrene D, camphene, and caryophyllene - which possess potent antioxidant and anti-inflammatory properties. These compounds help neutralize reactive oxygen species (ROS), reduce pro-inflammatory cytokine release, and promote collagen synthesis and epidermal regeneration, thereby mitigating UVB-induced oxidative stress and inflammatory responses (Budiman et al., 2024). These findings are consistent with previous studies on herbal essential oils. For example, Zyburtowicz et al. (2024) demonstrated that lavender essential oil reduces oxidative stress and DNA damage from UVB exposure, while Xu et al. (2025) reported that rosemary essential oil suppresses pro-inflammatory cytokines and enhances epidermal recovery. Similarly, Carson et al. (2006) found that tea tree essential oil downregulates collagen-degrading enzymes like MMP-1, and Perna et al. (2019) confirmed the anti-inflammatory and antioxidant effects of bergamot essential oil. Overall, EOCH shows comparable protective effects to standard treatments (e.g., VAP), underscoring its potential for use in dermatological and cosmeceutical products aimed at UV protection and skin repair.

3.3 Skin Moisture Analysis in EOCH-treated UVB-damaged Mice

Table 3 shows skin moisture percentages over time, highlighting the effects of EOCH on UVB-induced damage. The normal group maintained stable moisture levels (35.02±0.61% to 35.09±0.30%). In contrast, the UVB group's moisture dropped significantly from 34.88±0.83% at day 0 to 16.61±0.53% at week 4 ($p < 0.05$ vs. normal). The UVB + VAP group exhibited moderate recovery, with moisture rising from 26.98±0.48% on day 1 to 33.40±0.61% at week 4 ($p < 0.05$ vs. UVB), although still below normal levels. EOCH treatment improved hydration in a dose-dependent manner: the EOCH1 group increased from 22.53±0.32% on day 1 to 26.86±0.43% on week 4; the EOCH5 group from 24.12±0.70% to 29.15±0.31%; and the EOCH10 group from 25.96±0.29% to 31.85±0.34% at week 4, approaching normal values (all $p < 0.05$ vs. UVB).

The analysis of skin moisture levels in EOCH-treated UVB-damaged mice highlights EOCH's protective and restorative effects. UVB exposure disrupts the skin barrier, leading to excessive transepidermal water loss (TEWL) and impaired hydration, as evidenced by significant moisture depletion in untreated mice due to oxidative stress and inflammation (Hernández et al., 2019). In contrast, EOCH treatment improves hydration in a dose-dependent manner, with higher concentrations offering greater moisture restoration. This effect is attributed to EOCH's antioxidant and anti-inflammatory properties. By neutralizing reactive oxygen species (ROS), EOCH prevents lipid peroxidation and degradation of key skin barrier components such as ceramides and collagen, thereby reducing TEWL and supporting structural integrity (Jaffri, 2023). Additionally, its anti-inflammatory action suppresses pro-inflammatory cytokines that contribute to skin dryness and irritation (Pezantes-Orellana et al., 2024). These findings align with previous studies on herbal essential oils with skin-protective properties. For instance, research on Taif rose oil revealed its ability to ameliorate UVB-induced oxidative damage and skin inflammation, highlighting its antioxidant and anti-inflammatory properties (Abdallah et al., 2023). Similarly, a study on the photoprotective potential of geranium and calendula essential oils encapsulated in vesicular cream formulations found that these oils helped maintain the skin's natural antioxidant defense system and protected against UVB-induced damage (Lohani and Morganti, 2022). Additionally, research on *Artemisia sieversiana* essential oil demonstrated its efficacy in reducing UVB-induced photoaging in mice, attributed to its antioxidant activity and ability to inhibit collagen degradation (Zhou et al., 2021).

3.4 Antioxidant Effects of *Citrus hystrix* Peel Essential Oil in UVB-induced Skin Damage in Mice

Figure 2 demonstrates that EOCH treatment alleviates oxidative stress in UVB-damaged mice by lowering malondialdehyde (MDA, nmol/mL) and hydrogen peroxide (H_2O_2, nmol/g tissue) levels in the skin, liver, and kidney. UVB exposure significantly increased MDA (1.85 nmol/mL in skin, 2.79 in liver, 2.12 in kidney) and H_2O_2 (2.01 nmol/g in skin, 3.11 in liver, 2.25 in kidney) compared to normal controls ($p < 0.05$), indicating severe oxidative damage. EOCH treatment reduced both markers in a dose-dependent manner; the EOCH10 group showed the most pronounced effect by decreasing MDA to 1.24 nmol/mL (skin), 1.86 nmol/mL (liver), and 1.42 nmol/mL (kidney) and H_2O_2 to 1.33 nmol/g (skin), 2.08 nmol/g (liver), and 1.50 nmol/g (kidney) ($p < 0.05$).

Table 4 shows that UVB exposure significantly decreased glutathione (GSH) levels while increasing glutathione disulfide (GSSG) levels in the skin, liver, and kidney, thereby reducing the GSH/GSSG ratio and indicating oxidative stress. For instance, in the UVB group, GSH levels dropped to 2.41 μmol/mL (skin), 4.78 μmol/mL (liver), and 3.87 μmol/mL (kidney)

Table 5. Effects of *C. hystrix* DC. Peel Essential Oil on Glutathione Peroxidase (GPx), Glutathione Reductase (GR), and Thioredoxin (TRx) Levels in UVB-Induced Skin Damage in Mice

Experimental group	GPx level (U/mg protein)			GR level (U/mg protein)			TRx levels (μg/mg protein)		
	Skin	Liver	Kidney	Skin	Liver	Kidney	Skin	Liver	Kidney
Normal group	22.66± 0.19^{f}	48.33± 0.39^{f}	34.82± 0.81^{f}	24.75± 0.14^{f}	98.43± 0.41^{f}	55.31± 0.44^{f}	2.16± 0.10^{f}	8.95± 0.05^{f}	4.87± 0.06^{f}
UVB group	12.03± 0.21^{a}	26.85± 0.37^{a}	19.34± 1.05^{a}	13.75± 0.24^{a}	54.68± 0.38^{a}	30.73± 0.67^{a}	1.20± 0.12^{a}	4.97± 0.04^{a}	2.71± 0.07^{a}
UVB+VAP group	19.69± 0.42^{e}	43.94± 0.25^{e}	31.65± 0.12^{e}	22.50± 0.06^{e}	89.48± 0.72^{e}	50.28± 0.44^{e}	1.96± 0.10^{e}	8.14± 0.11^{e}	4.43± 0.05^{e}
UVB+EOCH1 group	14.44± 0.48^{b}	32.22± 1.08^{b}	23.21± 0.24^{b}	16.50± 0.49^{b}	65.62± 0.35^{b}	36.87± 0.62^{b}	1.44± 0.07^{b}	5.97± 0.05^{b}	3.25± 0.07^{b}
UVB+EOCH5 group	15.47± 0.22^{c}	34.52± 0.77^{c}	24.87± 0.33^{c}	17.68± 0.60^{c}	70.31± 0.52^{c}	39.51± 0.30^{c}	1.54± 0.05^{c}	6.39± 0.08^{c}	3.48± 0.11^{c}
UVB+EOCH10 group	18.05± 0.78^{d}	40.28± 0.57^{d}	29.02± 0.19^{d}	20.63± 0.62^{d}	82.03± 0.52^{d}	46.09± 0.48^{d}	1.80± 0.08^{d}	7.46± 0.04^{d}	4.06± 0.10^{d}

Values are expressed as Mean±SD; and letters (a, b, c, d, e, and f) represent the difference between groups ($p < 0.05$).

compared to 4.34, 8.61, and 6.97 in the normal group ($p < 0.05$), while GSSG levels rose significantly (0.22 nmol/mg in skin, 0.41 in liver, and 0.32 in kidney; $p < 0.05$). EOCH treatment restored GSH levels, reduced GSSG accumulation, and improved the GSH/GSSG ratio in a dose-dependent manner. The EOCH10 group, for example, increased GSH to 3.62 (skin), 7.18 (liver), and 5.81 (kidney) and decreased GSSG to 0.33 (skin), 0.62 (liver), and 0.48 (kidney), normalizing the GSH/GSSG ratio to 11.23 (skin), 11.62 (liver), and 12.34 (kidney) ($p < 0.05$).

Table 5 shows that UVB exposure significantly reduced the levels of glutathione peroxidase (GPx), glutathione reductase (GR), and thioredoxin reductase (TRx) in the skin, liver, and kidney compared to normal controls ($p < 0.05$). For example, GPx levels in the UVB group were 12.03 U/mg (skin), 26.85 U/mg (liver), and 19.34 U/mg (kidney), versus 22.66, 48.33, and 34.82 U/mg in the normal group. Similarly, GR and TRx levels were significantly lower in UVB-exposed tissues. EOCH treatment restored these enzyme levels in a dose-dependent manner. The EOCH10 group showed the most significant recovery, with GPx increasing to 18.05 U/mg (skin), 40.28 U/mg (liver), and 29.02 U/mg (kidney); GR rising to 20.63 U/mg (skin), 82.03 U/mg (liver), and 46.09 U/mg (kidney); and TRx improving to 1.80 μg/mg (skin), 7.46 μg/mg (liver), and 4.06 μg/mg (kidney) ($p < 0.05$).

The findings confirm that EOCH exhibits strong antioxidant potential in mitigating UVB-induced oxidative stress and skin damage. UVB exposure increases reactive oxygen species (ROS) such as hydrogen peroxide (H_2O_2), superoxide anion (O_2·-), and hydroxyl radicals (OH·), which trigger lipid peroxidation, protein oxidation, and DNA damage - contributing to skin barrier dysfunction, inflammation, and premature aging Nhung and Quoc (2024c). EOCH treatment significantly reduces oxidative stress markers, including malondialdehyde (MDA) and H_2O_2 levels, thereby protecting cellular structures by scavenging ROS and preventing further oxidative damage. This effect is largely attributed to its bioactive compounds, particularly monoterpenes and sesquiterpenes (Kim and Hong, 2024). Moreover, UVB exposure disrupts the glutathione (GSH) system by depleting GSH levels and increasing glutathione disulfide (GSSG), resulting in a decreased GSH/GSSG ratio that reflects impaired redox balance. EOCH effectively restores GSH levels, reduces GSSG accumulation, and improves the GSH/GSSG ratio—possibly through activation of the Nrf2-Keap1 signaling pathway, which regulates antioxidant enzyme expression and glutathione metabolism (Nhung and Quoc, 2024b). Supporting its efficacy further, EOCH significantly enhances the activities of key antioxidant enzymes such as glutathione peroxidase (GPx), glutathione reductase (GR), and thioredoxin reductase (TRx), which are crucial for detoxifying H_2O_2 and maintaining cellular redox balance. These results are consistent with previous studies on rosemary, tea tree, and bergamot essential oils, all of which have demonstrated similar benefits, including upregulation of glutathione metabolism, enhanced enzymatic antioxidant activity, and reduced lipid peroxidation (Carson et al., 2006; Perna et al., 2019; Xu et al., 2025). Overall, EOCH shows promise as a natural photoprotective agent for managing oxidative stress and preventing UVB-induced skin damage.

3.5 Immunomodulatory Effects of *Citrus hystrix* Peel Essential Oil in UVB-induced Skin Damage

Table 6 demonstrates that EOCH significantly mitigates UVB-induced inflammation and immune overactivation in a dose-dependent manner ($p < 0.05$). UVB exposure increased white blood cell (WBC) counts, neutrophil oxidative activity (NBT

Table 6. Effects of *C. hystrix* DC. Peel Essential Oil on White Blood Cell Count (WBC), Nitroblue Tetrazolium (NBT), and Total Immunoglobulin (TI) Levels in UVB-induced Skin Damage in Mice

Experimental group	WBC ($\times 10^3$ cell mm^{-3})		NBT (%)		TI (mg mL^{-1})	
	Blood	Skin	Blood	Skin	Blood	Skin
Normal group	5.85 ± 0.07^a	0.78 ± 0.04^a	15.61 ± 0.16^a	8.67 ± 0.06^a	14.86 ± 0.09^a	3.72 ± 0.04^a
UVB group	10.53 ± 0.22^f	1.41 ± 0.06^f	28.25 ± 0.53^f	15.61 ± 0.54^f	26.75 ± 0.48^f	6.69 ± 0.31^f
UVB+VAP group	6.44 ± 0.12^b	0.86 ± 0.02^b	17.17 ± 0.14^b	9.54 ± 0.26^b	16.35 ± 0.23^b	4.09 ± 0.04^b
UVB+EOCH1 group	8.78 ± 0.51^e	1.17 ± 0.09^e	23.42 ± 0.95^e	13.01 ± 0.45^e	22.29 ± 0.34^e	5.57 ± 0.20^e
UVB+EOCH5 group	8.19 ± 0.24^d	1.09 ± 0.04^d	21.85 ± 0.28^d	12.14 ± 0.38^d	20.95 ± 0.18^d	5.24 ± 0.32^d
UVB+EOCH10 group	7.02 ± 0.20^c	0.94 ± 0.04^c	18.73 ± 0.42^c	10.41 ± 0.82^c	17.83 ± 0.69^c	4.46 ± 0.07^c

Values are expressed as Mean±SD; and letters (a, b, c, d, e, and f) represent the difference between groups ($p < 0.05$).

reduction), and total immunoglobulin (TI) levels, contributing to skin damage and chronic inflammation. For instance, the UVB group showed WBC counts of 10.53×10^3 cells/mm^3 in blood and 1.41×10^3 cells/mm^3 in skin, compared to 5.85×10^3 cells/mm^3 and 0.78×10^3 cells/mm^3 in the normal group. EOCH treatment reduced these counts, with the EOCH10 group showing the greatest decrease (7.02×10^3 cells/mm^3 in blood and 0.94×10^3 cells/mm^3 in skin). Similarly, NBT reduction was elevated in UVB-exposed mice (28.25% in blood and 15.61% in skin) versus normal (15.61% in blood and 8.67% in skin), but EOCH10 reduced these values to 18.73% and 10.41%, respectively. TI levels were also significantly higher in the UVB group (26.75 mg/mL in blood and 6.69 mg/mL in the skin) compared to the normal group (14.86 mg/mL in blood and 3.72 mg/mL in the skin), and EOCH10 lowered them to 17.83 mg/mL and 4.46 mg/mL.

The results demonstrate that EOCH significantly enhances phagocytic activity by restoring both the phagocytic ratio (PR) and phagocytic index (PI) that are suppressed by UVB exposure (Figure 3). In the UVB group, PR decreased to 34.08% in blood and 22.57% in skin compared to 61.35% and 40.63% in normal controls ($p < 0.05$). EOCH treatment improved PR in a dose-dependent manner, with the EOCH10 group reaching 51.13% in blood and 33.86% in skin ($p < 0.05$). Similarly, the PI was significantly reduced in the UVB group (325 particles/-cell in blood and 216 particles/cell in skin versus 584 and 389 particles/cell in normals; $p < 0.05$. Additionally, UVB exposure induced excessive immune activation-evidenced by increased white blood cell counts, heightened neutrophil oxidative activity (NBT reduction), and elevated total immunoglobulin (TI) levels - which exacerbate.

These findings are consistent with previous studies. For instance, Pandur et al. (2021) showed that *Lavandula angustifolia* oil reduced UVB-induced inflammation by inhibiting IL-6 and TNF-α production; Pomi et al. (2023) reported that *Rosmarinus officinalis* oil enhanced antioxidant defenses and minimized DNA damage and Nova et al. (2024) demonstrated that *Melaleuca alternifolia* oil protected the epidermal barrier and maintained skin hydra.

4. CONCLUSIONS

In conclusion, *Citrus hystrix* peel essential oil (EOCH) effectively protects against UVB-induced damage in mice through multiple mechanisms. It improves skin condition and moisture retention while reducing oxidative stress by lowering MDA and H_2O_2 levels and restoring antioxidant enzyme activities (GPx, GR, TRx) and the GSH/GSSG ratio. Additionally, EOCH modulates the immune response by decreasing inflammation markers and enhancing phagocytic function, particularly at higher doses (EOCH10). These results support EOCH's potential as a natural therapeutic agent for preventing and treating UVB-induced skin damage.

5. ACKNOWLEDGEMENT

The authors sincerely thank Industrial University of Ho Chi Minh City for providing the necessary support to carry out this research. The authors are also deeply grateful to the animal research team at the Biotechnology Research Laboratory for their technical assistance and valuable expertise throughout the animal experimentation process.

REFERENCES

Abdallah, H. M., A. E. Koshak, M. A. Farag, N. S. E. Sayed, S. M. Badr-Eldin, O. A. A. Ahmed, M. M. Algandaby, A. B. Abdel-Naim, S. R. M. Ibrahim, G. A. Mohamed, P. Proksch, and H. Abbas (2023). Taif Rose Oil Ameliorates UVB-Induced Oxidative Damage and Skin Photoaging in Rats via Modulation of MAPK and MMP Signaling Pathways. *ACS Omega*, **8**(37); 33943–33954

Al-Sadek, T. and N. Yusuf (2024). Ultraviolet Radiation Biological and Medical Implications. *Current Issues in Molecular Biology*, **46**(3); 1924–1942

Ayubi, N., M. F. Halip, A. Komaini, M. S. Rifki, Nurkholis, M. Ridwan, M. N. B. Naharudin, D. A. Kusuma, Ilham, and D. T. Mario (2023). *Citrus limon* Has the Potential to Reduce Oxidative Stress and Inflammation After Physical Activity/Exercise: Systematic Review. *Retos*, **51**; 1168–1173

Basholli-Salihu, M., R. Schuster, A. Hajdari, D. Mulla,

H. Viernstein, B. Mustafa, and M. Mueller (2017). Phytochemical Composition, Anti-Inflammatory Activity, and Cytotoxic Effects of Essential Oils from Three *Pinus* spp. *Pharmaceutical Biology*, **55**(1); 1553–1560

Budiman, C., A. Miatmoko, V. E. P. S. Tyas, C. Ardianto, and D. Retnowati (2024). The Effects of Beta-Ionone Addition in Perfume on Behavior and Serum Cortisol Level of Stress-Induced Mice. *Science and Technology Indonesia*, **9**(2); 470–479

Carson, C. F., K. A. Hammer, and T. V. Riley (2006). *Melaleuca alternifolia* (Tea Tree) Oil: A Review of Antimicrobial and Other Medicinal Properties. *Clinical Microbiology Reviews*, **19**(1); 50–62

Chaudhary, P., P. Janmeda, A. O. Docea, B. Yeskaliyeva, A. F. A. Razis, B. Modu, D. Calina, and J. Sharifi-Rad (2023). Oxidative Stress, Free Radicals and Antioxidants: Potential Crosstalk in the Pathophysiology of Human Diseases. *Frontiers in Chemistry*, **11**; 1158198

Cioms and Iclas (2012). International Guiding Principles for Biomedical Research Involving Animals. Council for International Organization of Medical Sciences and the International Council for Laboratory Animal Science

Dourmishev, L. and D. Guleva (2021). Ultraviolet Diagnostic and Treatment Modalities in the Coronavirus Disease 2019 Pandemic. *Clinics in Dermatology*, **39**(3); 446–450

Fan, W., A. C. Rokohl, Y. Guo, H. Chen, T. Gao, V. Kakkassery, and L. M. Heind (2023). Narrative Review: Mechanism of Ultraviolet Radiation-Induced Basal Cell Carcinoma. *Frontiers of Oral and Maxillofacial Medicine*, **5**; 9–25

Fauzi, I., A. A. O. Farouk, and E. K. Perimal (2022). Antipruritic Properties of Topical *Channa striatus* Extract on Stratum Corneum Disruption-Itch Mice Model. *Neuroscience Research Notes*, **5**(3); 145

Fernando, P. D. S. M., M. J. Piao, K. A. Kang, H. M. U. L. Herath, E. T. Kim, C. L. Hyun, Y. R. Kim, and J. W. Hyun (2024). Butin Protects Keratinocytes from Particulate Matter 2.5 and Ultraviolet B-Mediated Damages. *Photodermatology, Photoimmunology and Photomedicine*, **40**(6); 13001

Ghani, A., S. Mohtashami, and S. Jamalian (2021). Peel Essential Oil Content and Constituent Variations and Antioxidant Activity of Grapefruit (*Citrus × paradisi* var. Red Blush) During Color Change Stages. *Journal of Food Measurement and Characterization*, **15**(6); 4917–4928

Gushiken, L. F. S., F. P. Beserra, M. F. Hussni, M. T. Gonzaga, V. P. Ribeiro, P. F. de Souza, J. C. L. Campos, T. N. C. Massaro, C. A. Hussni, R. K. Takahira, P. D. Marcato, J. K. Bastos, and C. H. Pellizzon (2022). Beta-Caryophyllene as an Antioxidant, Anti-Inflammatory and Re-Epithelialization Activities in a Rat Skin Wound Excision Model. *Oxidative Medicine and Cellular Longevity*; 9004014

He, X., X. Gao, and W. Xie (2024). Research Progress in Skin Aging and Immunity. *International Journal of Molecular Sciences*, **25**(7); 4101

Hernández, A. R., B. Vallejo, T. Ruzgas, and S. Björklund (2019). The Effect of UVB Irradiation and Oxidative Stress on the Skin Barrier—A New Method to Evaluate Sun Protection Factor Based on Electrical Impedance Spectroscopy. *Sensors*, **19**(10); 2376

Jaffri, J. M. (2023). Reactive Oxygen Species and Antioxidant System in Selected Skin Disorders. *Malaysian Journal of Medical Sciences*, **30**(1); 7–20

Kaur, C. D. and S. Saraf (2010). In Vitro Sun Protection Factor Determination of Herbal Oils Used in Cosmetics. *Pharmacognosy Research*, **2**(1); 22–25

Kim, H. J. and J. H. Hong (2024). Multiplicative Effects of Essential Oils and Other Active Components on Skin Tissue and Skin Cancers. *International Journal of Molecular Sciences*, **25**(10); 5397

Li, L., L. Chong, T. Huang, Y. Ma, Y. Li, and H. Ding (2023). Natural Products and Extracts from Plants as Natural UV Filters for Sunscreens: A Review. *Animal Models and Experimental Medicine*, **6**(3); 183–195

Li, Y., W. Li, Z. Ye, C. Ji, and Z. Zhou (2024). Antioxidant, Anti-Inflammatory, and Anticancer Activities of Five Citrus Peel Essential Oils. *Antioxidants*, **13**(12); 1562

Lin, F. R., X. X. Feng, C. W. Li, X. J. Zhang, X. T. Yu, J. Y. Zhou, X. Zhang, Y. L. Xie, Z. R. Su, and J. Y. X. Zhan (2014). Prevention of UV Radiation-Induced Cutaneous Photoaging in Mice by Topical Administration of Patchouli Oil. *Journal of Ethnopharmacology*, **154**; 408–418

Lohani, A. and P. Morganti (2022). Age-Defying and Photoprotective Potential of Geranium/Calendula Essential Oil Encapsulated Vesicular Cream on Biochemical Parameters Against UVB Radiation-Induced Skin Aging in Rat. *Cosmetics*, **9**; 43

Long, D. M., L. P. T. Quoc, T. T. P. Nhung, V. B. Thy, and N. L. Q. Nhu (2023). Chemical Profiles and Biological Activities of Essential Oil of *Citrus hystrix* DC. Peels. *Korean Journal of Food Preservation*, **30**(3); 395–404

Mardiyanto, M., I. Sholihah, and T. G. Jaya (2020). The Chitosan-Sodium Alginate Submicro Particles Loading Herbal of Ethanolic Extract of Leaves *Senna alata* L. for Curing of Bacterial Infection on Skin. *Science and Technology Indonesia*, **5**(3); 85–89

Nhung, T. T. P. and L. P. T. Quoc (2024a). Anti-Oxidative Stress and Immunosuppressive Effects of Ethanol Extract from *Sacha inchi* Leaves in Mice with CFA-Induced Rheumatoid Arthritis. *Tropical Journal of Natural Product Research*, **8**(9); 8584–8592

Nhung, T. T. P. and L. P. T. Quoc (2024b). Ethanol Extract of *Caryota urens* Lour Fruits Alleviates Oxidative Stress in a Murine Model of Rheumatoid Arthritis Induced by Freund's Complete Adjuvant. *Tropical Journal of Natural Product Research*, **8**(4); 6948–6956

Nhung, T. T. P. and L. P. T. Quoc (2024c). The Ethanol Extraction of *Gardenia stenophylla* Merr Fruit Mitigates Carbon Tetrachloride-Induced Hepatic Damage in Mice Through Modulation of Oxidative Stress and Immunosuppression. *International Journal of Agricultural Technology*, **20**(5); 2015–2034

Nova, B. G. V., L. D. S. Silva, M. D. S. Andrade, A. V. S. de Santana, L. C. T. da Silva, G. C. Sá, I. F. Zafred, P. H. D. A. Moreira, C. A. Monteiro, L. C. N. da Silva, and A. G. Abreu (2024). The Essential Oil of *Melaleuca alternifolia* Incorporated into Hydrogel Induces Antimicrobial and Anti-Inflammatory Effects on Infected Wounds by *Staphylococcus aureus*. *Biomedicine & Pharmacotherapy*, **173**; 116389

Nunes, K. C., D. Lazarin-Bidoia, T. Ueda-Nakamura, S. D. O. S. Lautenschlager, R. Michel, R. Auzély-Velty, and C. V. Nakamura (2025). Syringic Acid Protective Role: Combatting Oxidative Stress Induced by UVB Radiation in L-929 Fibroblasts. *Journal of Photochemistry and Photobiology B: Biology*, **264**; 113104

Nuryandani, E., E. Novitasari, M. F. Abdurrahman, N. Habibi, A. R. Sefrienda, D. Kurnianto, J. Jasmadi, and Y. Andriana (2024). Chemometric Analysis of GC-MS Chemical Profiles and Biological Activities of Three Citrus Essential Oils in Indonesia. *Journal of Applied Pharmaceutical Science*, **14**(12); 187–195

Pandur, E., A. Balatinácz, G. Micalizzi, L. Mondello, A. Horvát, K. Sipos, and G. Horváth (2021). Anti-Inflammatory Effect of Lavender (*Lavandula angustifolia* Mill.) Essential Oil Prepared During Different Plant Phenophases on THP-1 Macrophages. *BMC Complementary Medicine and Therapies*, **21**; 287

Perna, S., D. Spadaccini, L. Botteri, C. Girometta, A. Riva, P. Allegrini, G. Petrangolini, V. Infantino, and M. Rondanelli (2019). Efficacy of Bergamot: From Anti-Inflammatory and Anti-Oxidative Mechanisms to Clinical Applications as a Preventive Agent for Cardiovascular Morbidity, Skin Diseases, and Mood Alterations. *Food Science & Nutrition*, **7**(2); 369–384

Pezantes-Orellana, C., F. G. Bermúdez, C. M. De la Cruz, J. L. Montalvo, and A. Orellana-Manzano (2024). Essential Oils: A Systematic Review on Revolutionizing Health, Nutrition, and Omics for Optimal Well-Being. *Frontiers in Medicine*, **11**; 1337785

Pomi, F. L., V. Papa, F. Borgia, M. Vaccaro, A. Allegra, N. Cicero, and S. Gangemi (2023). *Rosmarinus officinalis* and Skin: Antioxidant Activity and Possible Therapeutical Role in Cutaneous Diseases. *Antioxidants*, **12**(3); 680

Siti, H. N., S. Mohamed, and Y. Kamisah (2022). Potential Therapeutic Effects of *Citrus hystrix* DC and Its Bioactive Compounds on Metabolic Disorders. *Pharmaceuticals*, **15**(2); 167

Stasiłowicz-Krzemień, A., D. Szymanowska, P. Szulc, and J. Cielecka-Piontek (2024). Antimicrobial, Probiotic, and Immunomodulatory Potential of *Cannabis sativa* Extract and Delivery Systems. *Antibiotics*, **13**(4); 369

Wei, M., X. He, N. Liu, and H. Deng (2024). Role of Reactive Oxygen Species in Ultraviolet-Induced Photodamage of the Skin. *Cell Division*, **19**; 1

Xu, J., T. Li, F. Li, H. Qiang, X. Wei, R. Zhan, and Y. Chen (2025). The Applications and Mechanisms of *Rosmarinus officinalis* L. in the Management of Different Wounds and UV-Irradiated Skin. *Frontiers in Pharmacology*, **15**; 1461790

Xu, X., Z. Ding, C. Pu, C. Kong, S. Chen, W. Lu, and J. Zhang (2024). The Structural Characterization and UV-Protective Properties of an Exopolysaccharide from a *Paenibacillus* Isolate. *Frontiers in Pharmacology*, **15**; 1434136

Yang, J., S. Y. Lee, S. K. Jang, K. J. Kim, and M. J. Park (2023a). Anti-Inflammatory Effects of Essential Oils from the Peels of Citrus Cultivars. *Pharmaceutics*, **15**(6); 1595

Yang, J. W., G. B. Fan, F. Tan, H. M. Kong, Q. Liu, Y. Zou, and Y. M. Tan (2023b). The Role and Safety of UVA and UVB in UV-Induced Skin Erythema. *Frontiers in Medicine*, **10**; 1163697

Zhang, P. C., Y. Hong, S. Q. Zong, L. Chen, C. Zhang, D. Z. Tian, D. Ke, and L. M. Tian (2023). Variation of Ferroptosis-Related Markers in HaCaT Cell Photoaging Models Induced by UVB. *Clinical, Cosmetic and Investigational Dermatology*, **16**; 3147–3155

Zhou, Y., L. He, N. Zhang, L. Ma, and L. Yao (2021). Photoprotective Effect of *Artemisia sieversiana* Ehrhart Essential Oil Against UVB-Induced Photoaging in Mice. *Photochemistry and Photobiology*, **98**(4); 958–968

Zyburtowicz, K., P. Bednarczyk, A. Nowak, A. Muzykiewicz-Szymańska, L. Kucharski, A. Wesołowska, and P. Ossowicz-Rupniewsk (2024). Medicinal Anti-Inflammatory Patch Loaded with Lavender Essential Oil. *International Journal of Molecular Sciences*, **25**(11); 6171

